

Towards Writing Style Adaptation in Handwriting Recognition

Jan Kohút (✉)^[0000-0003-0774-8903], Michal Hradiš^[0000-0002-6364-129X],
and Martin Kišš^[0000-0001-6853-0508]

Faculty of Information Technology, Brno University of Technology, Brno,
Czech Republic

{[ikohut](mailto:ikohut@fit.vutbr.cz), [ihradis](mailto:ihradis@fit.vutbr.cz), [ikiss](mailto:ikiss@fit.vutbr.cz)}@fit.vutbr.cz

Abstract. One of the challenges of handwriting recognition is to transcribe a large number of vastly different writing styles. State-of-the-art approaches do not explicitly use information about the writer’s style, which may be limiting overall accuracy due to various ambiguities. We explore models with writer-dependent parameters which take the writer’s identity as an additional input. The proposed models can be trained on datasets with partitions likely written by a single author (e.g. single letter, diary, or chronicle). We propose a Writer Style Block (WSB), an adaptive instance normalization layer conditioned on learned embeddings of the partitions. We experimented with various placements and settings of WSB and contrastively pre-trained embeddings. We show that our approach outperforms a baseline with no WSB in a writer-dependent scenario and that it is possible to estimate embeddings for new writers. However, domain adaptation using simple finetuning in a writer-independent setting provides superior accuracy at a similar computational cost. The proposed approach should be further investigated in terms of training stability and embedding regularization to overcome such a baseline.

Keywords: Handwritten text recognition · OCR · Domain adaptation · Domain dependent parameters · Finetuning · CTC.

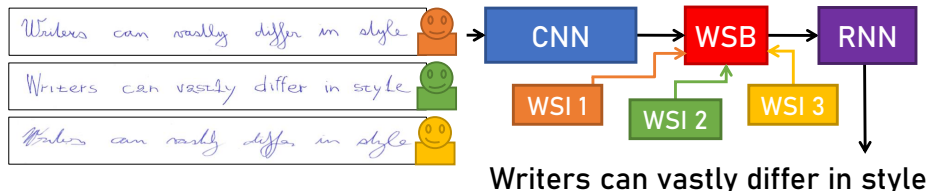


Fig. 1: Our proposed Writer Style Block (WSB) learns to utilize various writer styles based on writer style identifiers (WSI).

1 Introduction

Handwritten text of multiple writers can vastly differ in style, for example, the degree of slant, the way letters are joined (cursive or block letters), spacing between letters and words, similarity to printed text, the width of the stroke, etc. In fact, some characters may not be recognizable without the knowledge of the writer’s identity. To achieve sufficient text recognition accuracy, the state-of-the-art neural networks [24,19,2,6,16,10,30] must adapt to a large number of writer styles. While transcribing, these architectures have to rely only on the image of a text line, which may not provide sufficient context. The improper adaptation may lead to wrong interpretations of ambiguities, which naturally arise among multiple writers.

Figure 1 illustrates WS-Net, which is a standard CTC-based [24,19,2,6] architecture enhanced by our proposed Writer Style Block (WSB). Apart from the text line image, WS-Net takes an additional input in the form of a Writer Style Identifier (WSI). WSI serves as an index into a WSB writer style embedding table, where each writer is represented by a single embedding. WSB is an adaptive instance normalization [9] conditioned on the writer style embeddings. The adaptive instance normalization can modulate how the network processes information, which features become important and as such it provides WS-Net the ability to adapt to a vast amount of different writers.

The specific contributions of this paper are as follows: (1) Writer Style Block (WSB), an adaptive instance normalization conditioned by writer style embeddings, which can enhance any standard text handwritten recognition network with the ability to explicitly utilize writing styles in the training dataset; (2) extensive evaluation of WSB for various embedding dimensions 16–256, both in standard and pre-trained mode; (3) evaluation of WSB in writer-dependent and writer-independent scenarios.

2 Related Work

In the state-of-the-art approaches to handwritten text recognition, the writer’s identity information is usually not utilized. However, providing the recognition model with such information might be useful as the model can then better handle different writing styles, writer-specific patterns, etc. Closely related methods to the model adaptation, such as transfer learning, fine-tuning, and other similar techniques, are studied in several works [1,26,20,21,33,25], but the main disadvantage of these approaches is that they produce a unique model when adapted to a specific domain, which also needs to be clearly defined. More extensive model adaptation research can be found in the speech recognition area, where the focus is to efficiently adapt a model to a wide range of domains or even handle multiple data domains simultaneously. Our proposed Writer Style Block enhances a text recognition network to explicitly use the writer style information.

An approach similar to ours was proposed by Wang et al. [29] and it consists of two neural networks – writer style extractor network and text recognition

network. The architecture of both networks consists of convolutional blocks and recurrent layers. Local style representations obtained from the last recurrent layer of the writer style extractor network are aggregated by a mean pooling layer into a vector representing the global style of the text line. The writer style extractor network is trained to classify writers based on the global style representation. The global style representation and the local style representations are also aggregated by linear layers and connection operation into a single vector which is used for adaptation of the convolutional layers in the text recognition network.

When compared to our method, we don't extract the writer style representation in a feed-forward manner, but instead, we learned a fixed number of representative embeddings on the training dataset, which allowed the network to utilize all available writer style information while processing an individual text line image.

Text recognition has similar properties to automatic speech recognition (ASR). For this reason, we also present approaches to model adaptation from the field of ASR, where it is studied more extensively.

In ASR, model adaptation approaches are mainly focused on adapting a speaker-dependent (SD) part of a neural network, which represents given speaker identity, and keeping the rest of the network – the speaker-independent (SI) part – unchanged. In previous works, the adapted SI parts include the input layer (linear input network, LIN [18]), the hidden layer (linear hidden network, LHN [7]), and the output layer (linear output network, LON [13]). Such adaptation has several drawbacks, mainly the large number of adapted parameters which results in a slow adaptation process and model overfitting if strong regularization is not used. Also, as the speaker information is typically discarded in the latter layers of the network [17], in more recent approaches the SD parameters are located more toward the beginning of the network.

Many approaches aim to speed up the slow adaptation and to suppress the overfitting problems mentioned above by reducing the number of adapted SD parameters. Parametrization of activation functions with SD parameters was proposed by Zhang et al. [32]. In other works, the SD parameters are represented by scales and/or offsets in various layers. Namely, in Learning Hidden Unit Contributions (LHUC) [27], every kernel is followed by a SD scale parameter. Another option is to use the scales and offsets in batch normalization layers as the SD parameters [28,15]. Approaches by Zhao et al. [34,35] and Samarakoon et al. [22] propose to factorize weight matrices of SD linear layers as most of the information is stored in diagonals. Utilization of such decomposed matrices results fewer number of SD parameters.

Approaches proposed by Cui et al. [4] and Delcroix et al. [5] use an auxiliary SI network that generates SD parameters based on a small SD input (e.g. i-vector, learned speaker embedding, or similar features). In the first approach, the auxiliary network generates SD scales and offsets for hidden activations. The latter approach proposes to train a recognition network with several branches under the assumption that the different branches learn to specialize in different

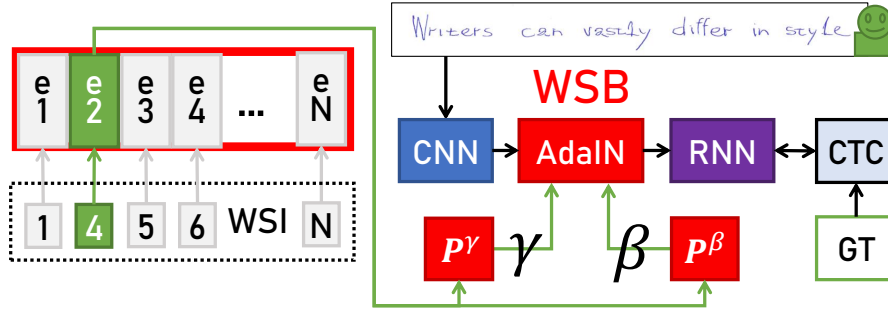


Fig. 2: Our proposed neural network consists of a convolutional part (CNN), a recurrent part (LSTM), and Writer Style Block (WSB).

types of speakers. The auxiliary network is then used to generate weights for aggregation of the outputs produced by the individual branches.

Some of the existing methods are focused on adapting the model without explicit speaker information. These methods usually extract the SD information from a longer utterance and utilize it locally. In the approach by Kim et al. [11], the model predicts activation offsets and scales of multiple layers from the utterance. Similarly, L. Sari et al. [23] use the utterance to predict local SD activation offsets by an auxiliary network. The approach by Xie et al. [31] is based on the LHUC approach mentioned above. They propose to produce the LHUC parameters in an online fashion by an auxiliary network.

3 Writer Style Block

We propose Writer Style Block (WSB), which allows WS-Net, described in detail in Section 5, to learn dedicated writer parameters in the form of writer style embeddings. Figure 2 shows WSB connected to WS-Net. The WSB is an adaptive instance normalization layer AdaIN [9]:

$$\text{AdaIN}(\mathbf{X}_c, \gamma_c, \beta_c) = \gamma_c \left(\frac{\mathbf{X}_c - \mu(\mathbf{X}_c)}{\sigma(\mathbf{X}_c) + \epsilon} \right) + \beta_c, \quad (1)$$

where \mathbf{X} , γ , β , μ , σ , ϵ stand for input, scales, offsets, mean, standard deviation and a small positive constant, c specifies the channel dimension. The adaptive scales γ and offsets β are given by two affine projections P^γ and P^β :

$$\gamma = P^\gamma(\mathbf{e}) = \mathbf{W}^\gamma \mathbf{e} + \mathbf{b}^\gamma, \beta = P^\beta(\mathbf{e}) = \mathbf{W}^\beta \mathbf{e} + \mathbf{b}^\beta, \quad (2)$$

where \mathbf{W}^γ , \mathbf{W}^β , \mathbf{b}^γ , \mathbf{b}^β are projection matrices and biases and \mathbf{e} is a writer style embedding specified by the corresponding Writer Style Identifier (WSI).

Therefore, in our architecture, each writer has dedicated parameters in the form of a writer style embedding \mathbf{e} , while all the other parameters are shared. While training, a writer style embedding \mathbf{e} is updated only on the respective writer training data, all the other parameters of WS-Net are updated on all writers.

Initialization. We initialize WSB similarly to the standard instance normalization. Each writer style embedding \mathbf{e} is initialized from the standard normal distribution $\mathcal{N}(0, 1)$. The projection matrices \mathbf{W}^γ , \mathbf{W}^β are initialized from a uniform distribution $\mathcal{U}(-\sqrt{\text{ED}} \times \tau, \sqrt{\text{ED}} \times \tau)$, where ED stands for embedding dimension and τ is a small positive constant. Conditioning the initialization on the square root of the ED results in the same standard deviation of the scales γ and the offsets β across all ED. The magnitude of this standard deviation can be manipulated with τ . In conducted auxiliary experiments we found that a reasonable value of the standard deviation is 0.1 and it is achieved by setting τ to 0.174. The \mathbf{b}^γ and \mathbf{b}^β are set to ones and zeros, respectively. For all ED, this way of initialization ensures, that both the scales γ and the offsets β have the same small standard deviation, while the scales are centered around 1 and the offsets around 0. Instead of initializing the embeddings from the standard normal distribution, pre-trained embeddings obtained by another approach can also be used. This approach is described in Section 6.

4 CzechHWR Dataset

Our dataset CzechHWR consists of triplets: a text line image, WSI, and the annotation of the text line image. It was created from three main sources: our OCR web application, a collection of Czech letters [8], and Czech chronicles. So far, users of the web application have uploaded and annotated documents containing about 295k handwritten text lines. Most of the documents were written in Czech modern cursive script, although, a marginal amount of documents in different scripts such as Gothic or German Kurrent is also present. They are mainly composed of military diaries, chronicles, letters, and notes. Based on document or page level manual inspection of the annotated documents, we assigned approximately 2.6k WSI. Czech letters is a collection of 2k letters, where the number of text lines is 87k. Most of them were written in Czech modern cursive, while a minimum amount was typeset. As it can be reasonably assumed that a handwritten letter has only one author, we assigned a distinct WSI to each letter. We manually annotated approximately 2 pages of 277 distinct Czech chronicles, resulting in 553 annotated pages with 24k text lines. As each page was chosen from a visually different place in the chronicle, we assigned a different WSI to each page.

The final CzechHWR dataset contains 406k annotated text line images with 5.1k WSI. The level of penmanship/readability differs, ranging from scribbles to calligraphy, although due to the origin of the data, the tendency is towards fairly readable texts (see the left side of Figure 3). There are two issues resulting from the WSI assigning process. First, there is no assurance that multiple WSI



Fig. 3: Left, samples from the CzechHWR dataset. Right, representative words of 19 target writers.

does not identify the same writer because it is not possible for the annotator to keep track of thousands of writing styles. Second, as we assigned the WSI on the document or page level, there is a possibility, that some text lines of the document/page belonged to distinct writers. The first issue should not present a problem for our system, as it will try to learn the same writer style embedding \mathbf{e} multiple times. The second issue should present only a slight regularization to the optimization process, as the vast majority of text lines were assigned correctly. The exact number of distinct writers is unknown, but a reasonable lower estimate is 4.5k. To avoid overcomplicated statements we often use “writer lines” to refer to data samples (triplets) that share the same WSI.

We divided the CzechHWR dataset for training and testing in the following way. We randomly draw 5k lines for testing (TST). The remaining lines were divided into seven clusters: 1, 22, 55, 110, 225, 550, and 1100, according to their writers (WSI). The cluster numbers specify the minimum number of lines for each writer to belong to that cluster. A writer belongs only to the cluster with the highest possible number, the resulting clusters are disjoint. Out of clusters 22, 55, 110, 225, 550, and 1100, for each writer (WSI), we respectively took 2, 5, 10, 25, 50, and 100 lines for testing clusters TST_C . The remaining lines formed the training clusters TRN_C . Out of convenience, we refer to both testing and training clusters with the minimum number of lines belonging to each writer in the training clusters: 1, 20, 50, 100, 200, 500, and 1000, e.g. TST_{20} or TRN_{500} . For example, a CER measured on TST_{50} set shows an error for writers that have at least 50 lines in the training dataset. The number of lines and WSI for each cluster is shown in Table 1, ALL stands for all clusters. For training, we merged all training clusters into a single training dataset (TRN). TST allows us to inspect the average CER because the distribution of WSI is the same as in TRN. TST_C and TRN_C clusters allow us to measure how the number of data samples per WSI affects the WSB performance.

Table 1: The number of lines and writers (WSI) for each cluster in the Czech-HWR dataset. For a detailed description, see the text.

	1	20	50	100	200	500	1000	ALL
TRN	13k	79k	82k	43k	24k	16k	122k	379k
TST	169	1k	1.1k	566	287	198	1.7k	5k
TST _w	0	4.5k	6.2k	3.2k	2k	1.1k	5.4k	22.4k
WSI	1.1k	2.3k	1.2k	322	79	21	54	5.1k

5 Writer Style Network

In this section, we describe the proposed WS-Net and its training procedure. We first introduce the baseline network architecture and later we specify the changes that lead to the proposed WS-Net.

The baseline architecture is similar to text recognition state-of-the-art architectures trained with CTC loss function [24,19,2,6]. It contains a convolutional part (CNN) and a recurrent part (RNN). The CNN part is a sequence of 4 convolutional blocks, where each has 2 convolutional layers with numbers of output channels set to 64, 128, 256, and 512, respectively. The input width subsampling factor of the CNN is 4. The RNN part processes three scaled versions of the WSB output with three branches, the scaling factors are 1, 0.5, and 0.25 and each branch has two LSTM layers. The outputs are upsampled back to the original resolution, summed, and processed with a final LSTM layer. Each LSTM layer is bidirectional and has a hidden feature size of 256 for each dimension. The output of the RNN block is processed by a final 1D convolutional layer. The baseline has 5 instance normalization layers, the first four are in the convolutional part behind each convolutional block, and the last is behind the recurrent block.

WS-Net enhances the baseline with WSB by replacing one or multiple standard instance normalization layers with adaptive instance normalization layers (AdaIN) conditioned on writer embeddings. Each AdaIN has its own projection matrices \mathbf{W}^γ , \mathbf{W}^β , and biases \mathbf{b}^γ , \mathbf{b}^β , but the writer style embeddings \mathbf{e} are shared. We experimented with two variants of WS-Net: Single AdaIN and All AdaIN. Single AdaIN is WS-Net, where the adaptive normalization layer (AdaIN) is behind the convolutional block (CNN), and all the rest are standard instance normalization layers. All AdaIN is WS-Net, where every normalization layer is AdaIN.

Motivation behind AdaIN placements. The motivation behind the AdaIN layer placement in Single AdaIN architecture is based on auxiliary experiments with All AdaIN architecture trained in multiple embedding dimension (ED) settings. By fixing scales and offsets for various AdaIN layers of a trained All AdaIN system, we simulated all possible settings of AdaIN layers. Out of all placements, we noticed a significantly higher drawback in performance for every setting where the AdaIN layer behind the CNN block was fixed, which suggests

that the All AdaIN system benefited most from this adaptive normalization layer. However, finding the best possible setting for AdaIN layers would mean training 31 different settings from scratch, for each embedding size ED. Additionally, we experimented with a setup where the AdaIN layer was behind the CNN and the RNN block, which turned up to be unstable and therefore we do not discuss the respective results in more detail.

5.1 Training

WS-Net is trained jointly with Adam optimizer [12], and the CTC loss function. The training data consists of triplets: a text line image, WSI, and the ground-truth transcription. Because the training samples are drawn randomly, embeddings that have more data samples assigned to them are updated more frequently. We mitigate this by normalizing embedding batch gradients by the frequency of their WSI in the batch.

We trained Single AdaIN and All AdaIN, with the embeddings initialized from the standard normal distribution (normal embeddings), for 500k iterations up until convergence. We used polynomial warmup of a third order to gradually increase the learning rate from 0 to 3×10^{-4} in 10k iterations. At iterations 200k and 400k, we used the warmup again, but the learning rate maximums were 7×10^{-5} and 1.75×10^{-5} . The batch size was set to 32. The baseline was trained in the same strategy.

Additionally, we trained Single AdaIN and All AdaIN, with the pre-trained embeddings (described in the following section), for 675k iterations in three consecutive steps. For each step, we trained the model up until convergence. First, we optimized all the parameters except the embeddings for 400k iterations. We used the warmup strategy in iterations 0, 200k, and 300k with the learning rate maximums being 3×10^{-4} , 1.5×10^{-4} , and 7×10^{-5} . Second, for the next 100k iterations, we optimized just the embeddings. We used the warmup strategy in iterations 400k and 450k and kept the learning rate the same. Third, for the final 175k iterations, we finetuned all the parameters. We used the warmup strategy in iterations 500k, 550k, 600k, and 650k with the learning rate maximums being 7×10^{-5} , 3×10^{-5} , and 1.5×10^{-5} . The model was significantly more accurate after each step.

We used data augmentation including color changes, noise, blur, and various geometric transformations to simulate different backgrounds, slants, spacing between characters, etc. Additionally, we mask the text line images with a random number of noise patches. The height of a noise patch is the same as the height of the text line image, the width is chosen randomly up to the height of the text line image forming at most a square patch. In this setting, the noise patch usually masks a maximum of two letters. The intuition behind masking is to strengthen the language modeling capability of the system.

6 Pre-training Writer Style Embeddings

Instead of using embeddings initialized from the standard normal distribution, we also use pre-trained ones. We implemented a contrastive learning approach, where the encoder is a stack of four convolutional layers with output channel dimensions 32, 64, 128, and 512 respectively, followed by three multi-head attention blocks with 4 heads and 512 channels, average pooling over the width dimension, and L2 normalization. The encoder generates an embedding \mathbf{q} for each text line image input. We used the normalized temperature-scaled cross entropy (NT-Xent) loss function [3]:

$$\mathcal{L}_{\mathbf{qp}} = -\log \frac{\exp(\mathbf{q} \cdot \mathbf{p}/\tau)}{\sum_{j=0}^N \exp(\mathbf{q} \cdot \mathbf{n}_j/\tau) + \exp(\mathbf{q} \cdot \mathbf{p}/\tau)}, \quad (3)$$

where \mathbf{q} forms a positive pair with the embedding \mathbf{p} , and negative pairs with embeddings \mathbf{n}_j . Embeddings of a positive pair are generated from image text lines belonging to the same writer. Embeddings of a negative pair are generated from image text lines of distinct writers. The final NT-Xent loss is given by $\mathcal{L} = \mu(\mathcal{L}_{\mathbf{qp}}), (\mathbf{q}, \mathbf{p}) \in \mathbf{P}$, where \mathbf{P} is a set of all positive pairs. As the final layer of the encoder is L2 normalization, the dot product will produce cosine similarity. The temperature parameter τ affects the strictness of the NT-Xent loss function. Values closer to 0 make it more strict, whereas higher values make it looser. Higher strictness force the encoder to produce closer cosine similarities, which means closer embeddings. We set τ to 0.15.

As the encoder can only provide an embedding \mathbf{q} for a text line image, we extract the final writer style embedding \mathbf{e} by aggregating output embeddings for 32 distinct and random text line images belonging to the respective writer. The aggregation is done by choosing the embedding \mathbf{q}_i which has the largest sum of above-average cosine similarities. The cosine similarity of two embeddings \mathbf{q}_i and \mathbf{q}_j is above average if it is larger than the average cosine similarity between all 32 embeddings. No data augmentation is used during the extracting process.

Training writer style encoder. The encoder was trained with AdamW [14] optimizer for 20k iterations, with a batch size of 180, and learning rate 2×10^{-4} . We use the same dataset as for the standard training, the augmentations are similar, but stronger, without any patch noise masking. The NT-Xent loss is evaluated for all positive pairs in the batch. We checked the convergence by visual inspection of text line images that belonged to the k nearest neighbors embeddings according to cosine similarity.

7 Writer-dependent Scenario

In this section, we describe the experiments conducted with the WS-Net on the CzechHWR dataset. Specifically, we compare Single AdaIN and All AdaIN variants of WS-Net to the baseline network. We trained architectures in both

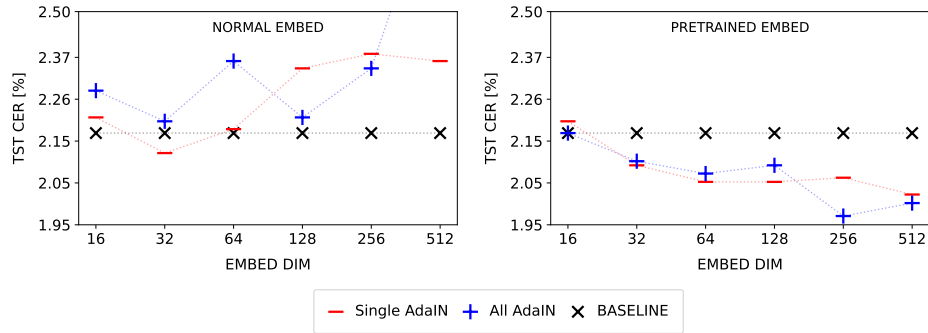


Fig. 4: Character error rate (CER) for Single AdaIN, All AdaIN, and the baseline on the test set. The graphs show CER for different embedding dimensions (ED) and for different initialization: randomly initialized (left) and pre-trained (right).

normal and pre-trained embedding setups for embedding dimensions (ED): 16, 32, 64, 128, 256, and 512, and a separate writer style encoder was trained for each ED. Figure 4 shows test character error (CER) for Single AdaIN, All AdaIN, and the baseline on the testing set TST. The left graph shows architectures initialized with normal embeddings. The Single AdaIN performed better for ED 16, 32, 64, and 512, and brought the best result for ED 32, All AdaIN was inconsistent across ED. All settings, except Single AdaIN with ED 32, brought worse performance than the baseline. The right graph shows architectures initialized with pre-trained embeddings. All settings consistently outperformed the baseline, with the exception of ED 16, which brought similar CER. Both AdaIN settings brought similar results, except for the ED 256, where All AdaIN had the lowest CER of all settings and decreased the test CER of the baseline by 9.22% relatively. All AdaIN is more stable across different ED, while initialized with pre-trained embeddings. When initialized with pre-trained embeddings, Single AdaIN brought progressively better performance with increasing ED, whereas initialization with normal embeddings had the opposite tendency since the ED 32.

Figure 5 shows Single AdaIN CER measured on various testing and training clusters (see Table 1 and Section 4) for ED 16, 32, and 256. The top graphs show the CER for Single AdaIN initialized with normal embeddings. We do not show the results for ED 64, 128, and 512, as the CER for ED 64 had the same tendency as ED 32, whereas ED 128 and 512 had the same tendency as ED 256. For larger clusters 100, 200, 500, and 1000, the test CER was smaller or similar to the baseline, while for smaller clusters 20 and 50, it was worse or similar. Only ED 32 and 64, outperformed the baseline for the larger clusters and evened out the baseline for smaller ones. As there was no noticeable relative decrease in train CER for smaller clusters (20, 50), the respective writer style embeddings probably overfitted in the wrong way and therefore brought poor generalization. Although we trained ED 256 up until convergence, the train CER suggests that

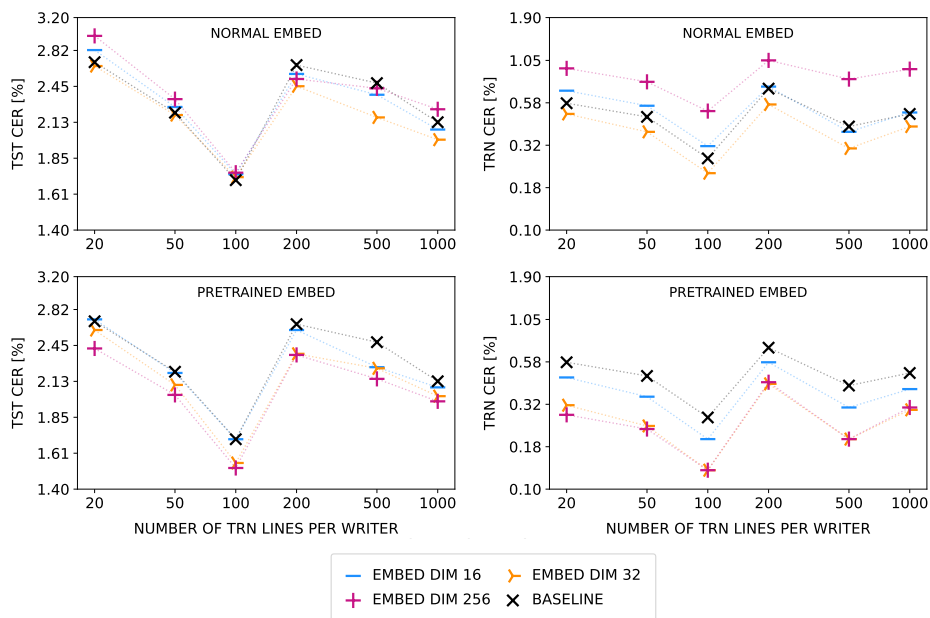


Fig. 5: Character error rate (CER) measured on various testing and training clusters for Single AdaIN with randomly initialized embeddings (top) and pre-trained embeddings (bottom).

it was not trained properly, as it should have overfit more than the smaller ED and the baseline (the same applied for ED 128 and 512).

The bottom graphs in Figure 5 show the results for Single AdaIN initialized with pre-trained embeddings. For all clusters, all ED except 16 had consistently smaller test CER than the baseline. The general tendency among all clusters, both for the testing and the training clusters, is that a higher ED has always lower CER than a smaller ED. Surprisingly, ED 16 brought significantly better performance for writers in cluster 500, this is probably due to the fact that the writer style encoder was able to find the unique properties of their writing styles and encode them even to smaller embeddings. Although all ED were fairly overfitted, they were able to generalize well among all the clusters.

The pre-trained embedding initialization variants generally outperformed the normal ones, while the largest differences were on smaller clusters. If we compare the best ED out of each variant, ED 32 for normal embeddings to ED 256 for pre-trained embeddings, we can see that the latter was better only on the smaller clusters. Single AdaIN trained from scratch (initialized with normal embeddings) does not guarantee in any way that the learned embeddings would represent the respective writer styles and therefore it is prone to overfit on writer irrelevant details, especially for smaller amount of writer lines. On the other hand, Single AdaIN initialized with the pre-trained embeddings is forced to learn the proper utilization of writer styles in relation to the handwritten text recognition task,

as the pre-trained embeddings are fixed for the first 400k training iterations. As the writer style encoder was directly trained to encode the writer style, it learned to extract robust and representative embeddings even for writers from smaller clusters.

For pre-trained embeddings and normal embeddings with ED 128 and 256, the t-SNE projections showed semantically meaningful clusters, where writers of similar scripts were grouped together. For normal embeddings with ED 16, 32, and 64, the projections did not show visible clusters.

8 Writer-independent Scenario

For new writers, our architecture cannot be used in a simple feed-forward manner. However, as all parameters except the writer style embeddings are shared among the writers, we should be able to adapt to a new writer by finding a new representative embedding. We experimented with two approaches. The first selected the new embedding out of the existing ones according to CER on adaptation lines. As there are more than 5k existing embeddings, we clustered the existing embedding space with the k-mean algorithm into 50 clusters and evaluated only one random embedding from each cluster. The second optimized a new embedding with the 150 LBFSG iterations, the adaptation text line images were augmented in the same way as the training ones. To inspect the quality of selection and optimization for different numbers of adaptation lines, we define writer adaptation runs. A writer adaptation run consists of adapting the respective writer on 5 line clusters: 16, 32, 64, 128, and 256, where the numbers refer to the number of lines in them, a smaller cluster is always a subset of a larger one, and the lines of the largest cluster are drawn randomly from all available lines. We run 23 adaptation runs for 19 new writers and 3 fully-trained Single AdaIN architecture setups: normal embeddings with ED 32, pre-trained embeddings with ED 32, and pre-trained embeddings with ED 256, resulting in final $23 \times 19 \times 3$ runs for both the selection and optimization approach. We always chose the best-performing embedding on the adaptation lines and inspected CER on test lines, there are 256 randomly drawn testing lines for each adaptation run.

The selection approach performed worse than the baseline even for higher amounts of adaptation lines. Generally, for all Single AdaIN setups, the selection was more accurate for higher numbers of adaptation lines. Surprisingly, the best-performing setup of Single AdaIN was normal embeddings ED 32, while for some writers and selections based on 256 adaptation lines, it performed similarly to the baseline. We do not show detailed results, as it did not outperform the baseline and we did not notice any interesting properties apart from the already described. For the optimization approach, we tried to optimize from the selected embeddings, but the mean of the existing ones turned out to be a better starting point.

Figure 6 shows the performance of our optimization approach expressed as relative test CER reductions of the baseline. A boxplot represents the distribution of the 19 writers' CER reductions, and a writer's CER reduction is the

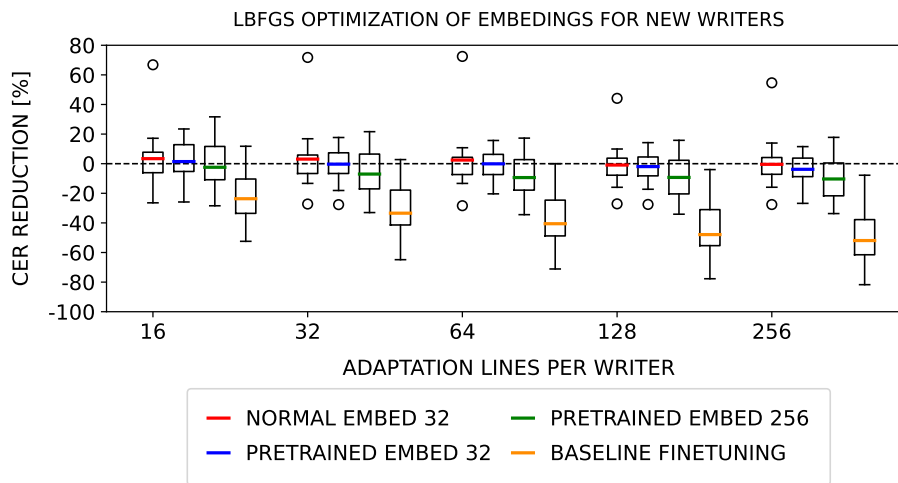


Fig. 6: The performance of our optimization approach expressed as relative test CER reductions of the baseline compared to baseline finetuning.

mean of the writer’s CER reductions measured on 23 runs. More precisely, the CER reduction is given by:

$$\frac{A - B}{B}, \quad (4)$$

where A is the test CER of the adapted Single AdaIN, and B is the test CER of the baseline. Generally, for all Single AdaIN setups, the optimization was more accurate for higher numbers of adaptation lines. By further inspecting the results in relation to Figure 3, we noticed that the performance varied across writers in relation to their scripts. CER reductions were largest for scripts that were not sufficiently represented in the CzechHWR dataset, such as German Kurrent or Ghotic, while the performance worsen for the CzechHWR-like scripts. On average, the pre-trained embeddings ED 256 setup provided the best performance, although it performed worse than the respective ED 32 setup for some writers. The normal embeddings ED 32 setup brought the lowest CER reductions, while it vastly worsen the performance for some writers.

Based on these results, WS-Net is able to learn writer style space that can significantly boost the transcription accuracy of new writers, however, finding representative embeddings is not straightforward. We argue that this is to some extent caused by the sensitivity of WS-Net to precise writer style embeddings. We evaluated the sensitivity of WS-Net by randomly shuffling WSI in testing datasets, the test CER increased 2 times for the normal setting and 4 times for the pre-trained setting. Therefore, simply selecting an existing embedding brought worse performance for all new writers, as WS-Net was too overfitted to existing writers and none of them had an extremely similar style to the new

ones. Optimization was difficult and unstable, as both the mean and the selected embeddings did not provide a good starting point.

Note that for Single AdaIN pre-traiend ED 256 setup we evaluated WS-Net with embeddings provided by the writer style encoder in an unsupervised manner, both without and with further optimization, but the results were comparable to supervised selection and optimization from the mean. Furthermore, as the embeddings might have slightly changed in the last phase of the training, we tried to boost the performance of this approach by finetuning the writer style encoder on the WS-Net writer style embeddings using the L2 loss, but even this setup failed.

So far, the only reasonable solution for new writers is to find representative embeddings with optimization on larger numbers of adaptation lines, however for such scenarios, a simple finetuning of the baseline brought significantly better test CER reductions. Note that we estimated the optimal number of finetuning iterations with 4-fold cross-validation. So far, WS-Net is only suitable for the writer-dependent scenario where it consistently outperformed the baseline, whereas it is not a suitable choice for writer-independent scenarios, especially if enough annotated data for new writers are available.

In our future work, we plan to redesign the WSB block, so it can be used in writer-independent scenarios without any adaptation lines. The idea is based on an attention mechanism, which would take the hidden features of the processed text line image as queries, and embeddings of the writer style space as keys and values.

9 Conclusion

We showed that a standard CTC-based neural network enhanced by proposed Writer Style Block (WSB) can utilize a vast number of writing styles. While initializing WSB with embeddings pre-trained in an unsupervised contrastive manner, the enhanced architecture was able to consistently outperform the baseline version even for writers that were poorly represented in the training set. On the other hand, training the WSB writer style embeddings from scratch, led to worse performance on average. Although we were unable to find an appropriate way to estimate representative embeddings for new writers, we confirmed their existence in the WSB writer style embedding space by optimization on 256 adaptation lines. This suggests that the WSB provides superior performance even for new writers. In future work, we plan to learn the appropriate estimation in a supervised manner by extending the WSB with an attention mechanism, which would take the hidden features of a processed text line image as queries and the writer style embeddings as keys and values.

References

1. Aradillas, J.C., Murillo-Fuentes, J.J., Olmos, P.M.: Boosting offline handwritten text recognition in historical documents with few labeled lines. *IEEE Access* **9**, 76674–76688 (2021)

2. Bluche, T., Messina, R.: Gated convolutional recurrent neural networks for multilingual handwriting recognition. In: 2017 14th IAPR International Conference on Document Analysis and Recognition (ICDAR). vol. 01, pp. 646–651 (2017). <https://doi.org/10.1109/ICDAR.2017.111>
3. Chen, T., Kornblith, S., Norouzi, M., Hinton, G.: A simple framework for contrastive learning of visual representations. In: International conference on machine learning. pp. 1597–1607. PMLR (2020)
4. Cui, X., Goel, V., Saon, G.: Embedding-based speaker adaptive training of deep neural networks. CoRR **abs/1710.06937** (2017)
5. Delcroix, M., Kinoshita, K., Ogawa, A., Huemmer, C., Nakatani, T.: Context adaptive neural network based acoustic models for rapid adaptation. IEEE/ACM Transactions on Audio, Speech, and Language Processing **26**(5), 895–908 (2018)
6. Dutta, K., Krishnan, P., Mathew, M., Jawahar, C.V.: Improving cnn-rnn hybrid networks for handwriting recognition. In: 2018 16th International Conference on Frontiers in Handwriting Recognition (ICFHR). pp. 80–85 (2018). <https://doi.org/10.1109/ICFHR-2018.2018.00023>
7. Gemello, R., Mana, F., Scanzio, S., Laface, P., De Mori, R.: Linear hidden transformations for adaptation of hybrid ann/hmm models. Speech Communication **49**(10-11), 827–835 (2007)
8. Hladká, Z.: 111 let českého dopisu v korpusovém zpracování (2013)
9. Huang, X., Belongie, S.J.: Arbitrary style transfer in real-time with adaptive instance normalization. CoRR **abs/1703.06868** (2017)
10. Kang, L., Riba, P., Rusiñol, M., Fornés, A., Villegas, M.: Pay attention to what you read: non-recurrent handwritten text-line recognition. Pattern Recognition **129**, 108766 (2022)
11. Kim, T., Song, I., Bengio, Y.: Dynamic layer normalization for adaptive neural acoustic modeling in speech recognition. CoRR **abs/1707.06065** (2017)
12. Kingma, D.P., Ba, J.: Adam: A method for stochastic optimization. In: Bengio, Y., LeCun, Y. (eds.) ICLR 2015, San Diego, CA, USA, May 7-9, 2015, Conference Track Proceedings (2015)
13. Li, B., Sim, K.C.: Comparison of discriminative input and output transformations for speaker adaptation in the hybrid nn/hmm systems. In: Eleventh Annual Conference of the International Speech Communication Association (2010)
14. Loshchilov, I., Hutter, F.: Fixing weight decay regularization in adam. CoRR **abs/1711.05101** (2017), <http://arxiv.org/abs/1711.05101>
15. Mana, F., Weninger, F., Gemello, R., Zhan, P.: Online batch normalization adaptation for automatic speech recognition. In: IEEE ASRU 2019. pp. 875–880. IEEE (2019)
16. Michael, J., Labahn, R., Grüning, T., Zöllner, J.: Evaluating sequence-to-sequence models for handwritten text recognition. In: 2019 International Conference on Document Analysis and Recognition (ICDAR). pp. 1286–1293. IEEE (2019)
17. Mohamed, A.r., Hinton, G., Penn, G.: Understanding how deep belief networks perform acoustic modelling. In: IEEE ICASSP 2012. pp. 4273–4276. IEEE (2012)
18. Neto, J., Almeida, L., Hochberg, M., Martins, C., Nunes, L., Renals, S., Robinson, T.: Speaker-adaptation for hybrid hmm-ann continuous speech recognition system (1995)
19. Puigcerver, J.: Are multidimensional recurrent layers really necessary for handwritten text recognition? In: 2017 14th IAPR International Conference on Document Analysis and Recognition (ICDAR). vol. 01, pp. 67–72 (2017). <https://doi.org/10.1109/ICDAR.2017.20>

20. Reul, C., Tomasek, S., Langhanki, F., Springmann, U.: Open source handwritten text recognition on medieval manuscripts using mixed models and document-specific finetuning. In: Document Analysis Systems: 15th IAPR International Workshop, DAS 2022, La Rochelle, France, May 22–25, 2022, Proceedings. pp. 414–428. Springer (2022)
21. Reul, C., Wick, C., Nöth, M., Büttner, A., Wehner, M., Springmann, U.: Mixed model ocr training on historical latin script for out-of-the-box recognition and finetuning. In: The 6th International Workshop on Historical Document Imaging and Processing. pp. 7–12 (2021)
22. Samarakoon, L., Sim, K.C.: Factorized hidden layer adaptation for deep neural network based acoustic modeling. *IEEE/ACM Transactions on Audio, Speech, and Language Processing* **24**(12), 2241–2250 (2016)
23. Sarı, L., Thomas, S., Hasegawa-Johnson, M., Picheny, M.: Speaker adaptation of neural networks with learning speaker aware offsets. *Interspeech* (2019)
24. Shi, B., Bai, X., Yao, C.: An end-to-end trainable neural network for image-based sequence recognition and its application to scene text recognition. *CoRR* **abs/1507.05717** (2015), <http://arxiv.org/abs/1507.05717>
25. Soullard, Y., Swaileh, W., Tranouez, P., Paquet, T., Chatelain, C.: Improving text recognition using optical and language model writer adaptation. In: *ICDAR 2019*. pp. 1175–1180 (2019)
26. Soullard, Y., Swaileh, W., Tranouez, P., Paquet, T., Chatelain, C.: Improving text recognition using optical and language model writer adaptation. In: 2019 International Conference on Document Analysis and Recognition (ICDAR). pp. 1175–1180. IEEE (2019)
27. Swietojanski, P., Li, J., Renals, S.: Learning hidden unit contributions for unsupervised acoustic model adaptation. *CoRR* **abs/1601.02828** (2016)
28. Wang, Z.Q., Wang, D.: Unsupervised speaker adaptation of batch normalized acoustic models for robust asr. In: *IEEE ICASSP 2017*. pp. 4890–4894. IEEE (2017)
29. Wang, Z.R., Du, J.: Fast writer adaptation with style extractor network for handwritten text recognition. *Neural Networks* **147**, 42–52 (2022). <https://doi.org/https://doi.org/10.1016/j.neunet.2021.12.002>, <https://www.sciencedirect.com/science/article/pii/S0893608021004755>
30. Wick, C., Zöllner, J., Grüning, T.: Transformer for handwritten text recognition using bidirectional post-decoding. In: Document Analysis and Recognition–ICDAR 2021: 16th International Conference, Lausanne, Switzerland, September 5–10, 2021, Proceedings, Part III. pp. 112–126. Springer (2021)
31. Xie, X., Liu, X., Lee, T., Wang, L.: Fast dnn acoustic model speaker adaptation by learning hidden unit contribution features. In: *INTERSPEECH*. pp. 759–763 (2019)
32. Zhang, C., Woodland, P.C.: Parameterised sigmoid and relu hidden activation functions for dnn acoustic modelling. In: *Sixteenth Annual Conference of the International Speech Communication Association* (2015)
33. Zhang, Y., Nie, S., Liu, W., Xu, X., Zhang, D., Shen, H.T.: Sequence-to-sequence domain adaptation network for robust text image recognition. In: *Proceedings of the IEEE/CVF Conference on Computer Vision and Pattern Recognition*. pp. 2740–2749 (2019)
34. Zhao, Y., Li, J., Gong, Y.: Low-rank plus diagonal adaptation for deep neural networks. In: *IEEE ICASSP 2016*. pp. 5005–5009. IEEE (2016)
35. Zhao, Y., Li, J., Kumar, K., Gong, Y.: Extended low-rank plus diagonal adaptation for deep and recurrent neural networks. In: *IEEE ICASSP 2017*. pp. 5040–5044. IEEE (2017)